ELSEVIER

www.elsevier.nl/locate/jorganchem

Journal of Organometallic Chemistry 585 (1999) 266–274

Journal of Organometallic Chemistry

Reactivity studies of trimethylaluminum, trimethylgallium, and trimethylindium with a series of five silylamines: molecular structure of *trans*-$[Me_2InN(Me)SiMe_3]_2$

Eric K. Styron, Steven J. Schauer, Charles H. Lake, Charles L. Watkins [1], Larry K. Krannich *

Department of Chemistry, University of Alabama at Birmingham, Birmingham, AL 35294-1240, USA

Received 5 February 1999

Abstract

Equimolar mixtures of Me_3M (M = Al, Ga, In) with five silylamines, $N(SiMe_3)_3$, $HN(SiMe_3)_2$, $MeN(SiMe_3)_2$, Me_2NSiMe_3, and $HN(Me)SiMe_3$, were prepared in benzene-d_6 and toluene-d_8 solutions and variable temperature ^{1}H- and ^{13}C-NMR spectroscopy was utilized to deduce the capacity of these systems to form stable complexes under varying degrees of amine silylation. Approximate values for the cone angles of the bound amines are extrapolated from NMR data and from literature trends. The 1,2-elimination reactions of MMe_3 with $HN(Me)SiMe_3$ at 90°C (120°C for the Ga analogue) afford mixtures in solution of *cis*- and *trans*-$[Me_2MN(Me)SiMe_3]_2$ which crystallizes in the *trans* form. In solution, the dimers equilibrate to mixtures of *cis* and *trans* geometrical isomers. The *trans* isomer is the predominant isomer for all three analogues. The equilibration process follows reversible first-order kinetics for each dimer. The thermodynamic and kinetic parameters for the *trans* to *cis* equilibration have been determined and are discussed in terms of an intramolecular ring opening mechanism. The molecular structure of *trans*-$[Me_2InN(Me)SiMe_3]_2$ has been determined by a single crystal X-ray diffraction study. The molecule is dimeric and lies on a crystallographic center of symmetry.

Keywords: Silylamine; Structure; NMR; Isomerization; Kinetics; Thermodynamics

1. Introduction

The reactivity of trialkylaluminum, -gallium, and -indium toward alkyl amines to form datively bonded complexes is well documented [1–15]. Recently, our research group reported the results of a study of the reactions of trimethylaluminum, -gallium, and -indium toward a series of thirteen secondary amines to yield three series of room temperature (r.t.) stable adducts [9,15]. The ^{1}H- and ^{13}C-NMR data for all three series of adducts indicate a correlation between the chemical shifts of the methyl groups on the metal and the relative steric requirements of the amines. Plots of the ^{13}C chemical shifts of the methyl group on the metal versus the cone angles of the free amines were linear below an angle of 138°. Three amines with cone angles greater than 138° gave chemical shift data farther upfield than expected. Correlation of the chemical shift data for $HNBu^i_2$, $HNBu^s_2$, and $HN(CH_2Ph)_2$ with the corresponding data for the less sterically hindered amines suggests a reduction in their cone angle upon complex formation via their internal degrees of freedom, similar to that reported for $Me_3Al{\cdot}P(CH_2Ph)_3$ in a study of adducts formed between Me_3Al and tertiary phosphines [16].

In order to investigate further the influence of the steric nature of the amine on the ^{1}H- and ^{13}C-NMR data for a given complex, variable temperature ^{1}H- and ^{13}C-NMR spectra were obtained on 1:1 mixtures of Me_3Al, Me_3Ga, and Me_3In with a series of five silylamines in benzene-d_6 and toluene-d_8 solutions. This series of silylamines, $N(SiMe_3)_3$, $HN(SiMe_3)_2$, $MeN(SiMe_3)_2$, Me_2NSiMe_3, and $HN(Me)SiMe_3$, were chosen to give a wide range of variation in steric hindrance and amine geometry. The NMR chemical

* Corresponding author.
[1] Also corresponding author.

0022-328X/99/$ - see front matter
PII: S0022-328X(99)00234-X

shift data for each of the mixtures versus those of the free reagents were analyzed in terms of possible complex formation, the influence of the number of Me_3Si– groups in the amine upon complex formation, and, for those mixtures where strong adduct formation was noted, a correlation with the chemical shift-cone angle trends for the analogous alkylamine systems.

Thermolysis of 1:1 mole ratio mixtures of the unsymmetric silylamine, $HN(Me)SiMe_3$, with Me_3Al, Me_3Ga, and Me_3In yielded the respective dimers, $[Me_2AlN(Me)SiMe_3]_2$ (**1**), $[Me_2GaN(Me)SiMe_3]_2$ (**2**), and $[Me_2InN(Me)SiMe_3]_2$ (**3**). In solution each of the dimers exists as a *cis–trans* isomeric mixture. ^{1}H-NMR spectra were obtained as a function of temperature and time for each of the three dimers and the thermodynamic and kinetic parameters for the *trans–cis* equilibration process were determined. These results, which suggest an intramolecular ring opening mechanism consisting of the breaking of the metal–nitrogen bond, followed by rotation about the metal–nitrogen bond and rebridging, are compared and contrasted with data reported for the compounds $[Me_2AlN(Me)C_6H_5]_2$ [17,18], $[Me_2GaN(Me)C_6H_5]_2$ [18], $[Me_2InN(Me)C_6H_5]_2$ [18], $[Me_2GaN(H)Bu^t]_2$ [19], and $[Me_2AlN(H)Bu^t]_2$ [20].

The molecular structure of **3** in the solid state has been obtained by single-crystal X-ray studies. The $[InN]_2$ four-membered ring is planar with the NMe and $NSiMe_3$ groups in the *trans* conformation. The molecular structure data for **3** is discussed and compared with reported structures for other aminoindane dimers.

2. Experimental

2.1. General experimental conditions

Compound syntheses and sample preparation procedures were performed using a Vacuum Atmospheres Model HE-43 Dri-Lab outfitted with a model HE-493 Dri-Train or under an atmosphere of dry nitrogen using standard Schlenk and vacuum-line techniques. Trimethylaluminum, Texas Alkyls, was used as obtained. Trimethylgallium, Morton Advanced Materials, was distilled under vacuum and the purity checked by NMR prior to use. Trimethylindium, Morton Advanced Materials, was sublimed and the purity checked by NMR prior to use. The amines in this study were purchased from Aldrich Chemicals, Inc. except $HN(Me)SiMe_3$, which was synthesized by the reaction of trimethylsilyl chloride with methylamine [21]. Benzene-d_6 and toluene-d_8 were purchased from Aldrich Chemicals, Inc. and stored over molecular sieves. All ^{1}H- and ^{13}C-NMR data for the mixtures were recorded on a Bruker ARX 300 FT-NMR spectrometer. Complex formation studies were performed on 0.20 M benzene-d_6 solutions and the chemical shifts were referenced to those of the solvent. All 2-D NOESY NMR and equilibration studies spectra were run using a Bruker DRX 400 FT-NMR spectrometer on 0.10 M solutions. Melting points were obtained in capillaries under nitrogen and are uncorrected. Elemental analyses were performed by E&R Microanalytical Laboratory, Inc., Parsippany, NJ.

2.2. Preparation of mixtures for assessment of complex formation

Equimolar mixtures of Me_3M (M = Al, Ga, In) and a series of five silylamines and solutions of the individual reagants were prepared in benzene-d_6 at a concentration of 0.20 M. Variable temperature ^{1}H- and ^{13}C-NMR spectra were then obtained over the range 24–63°C. Low temperature data were collected at −33°C on toluene-d_8 solutions. Changes in the ^{1}H- and ^{13}C-NMR chemical shifts of the mixtures versus those of the free reagents were used as evidence of complex formation. The chemical shift values of the free reagents at a given temperature were subtracted from those of the mixtures at that temperature ($\Delta\delta = \delta(\text{mixture}) - \delta(\text{free})$).

2.3. Synthesis of dimers of the form $[Me_2MN(Me)SiMe_3]_2$ where M = Al, Ga, and In

Dimeric derivatives were prepared by thermolysis of $Me_3M{\cdot}NH(Me)SiMe_3$. In each case the complex was formed in toluene and heated in a high pressure reaction tube until gas (methane) evolution ceased. The aluminum (**1**) and indium (**3**) reaction mixtures were heated at 90°C, while the gallium (**2**) analogue required a temperature of 120°C. The synthesis and analytical data for **1** have been reported [21,22]. The thermolysis of the adducts leads to formation of a mixture of *trans* (**a**) and *cis* (**b**) isomers in ratios of approximately 2.5:1, respectively. However, recrystallization from toluene by removal of solvent yields crystals of the *trans* isomer in each case, as evidenced by X-ray data for **3** and ^{1}H-NMR data of solutions of **1** and **2** obtained as quickly as possible after mixing.

2.4. H-NMR studies of the trans to cis isomerization of $[Me_2MN(Me)SiMe_3]_2$

For each study, a 0.10 M solution of the respective dimer was prepared in toluene-d_8 and placed in a 5 mm NMR tube. The tube was then inserted into the NMR probe which had been equilibrated at a specific temperature setting for approximately 30 min. The sample was thermally equilibrated in the probe for approximately 15 min before beginning the experiment. The experiment consisted of obtaining ^{1}H spectra at timed intervals and monitoring the integral ratio for the resonance signals exhibited by the methyl groups attached to the

nitrogen. All three reactions displayed reversible first-order kinetics through a general plot of $-\ln(1-[cis]/[cis]_{eq})$ versus time. Selected experiments for **2** and **3** were conducted at 0.050 M concentration in order to determine if any concentration dependent processes were present. The gallium and indium analogues isomerized relatively rapidly so K_{eq} values could be determined at the end of the respective experiment. However, determination of the K_{eq} values for the aluminum species required the use of a temperature controlled bath followed by a ^{1}H-NMR spectrum in a probe thermally equilibrated at the respective temperature.

2.5. Characterization of $[Me_2AlN(Me)SiMe_3]_2$, $[Me_2GaN(Me)SiMe_3]_2$, and $[Me_2InN(Me)SiMe_3]_2$

2.5.1. $[Me_2AlN(Me)SiMe_3]_2$ (**1**) [21,22]

M.p. 74–76 (69°C) [21]. ^{1}H-NMR (**1a**): δ −0.45 (s, 12H, $AlCH_3$), 2.33 (s, 6H, NCH_3), 0.14 (s, 18H, $SiCH_3$); ^{1}H-NMR (**1b**): δ −0.50 (s, 6H, $AlCH_3$), −0.36 (s, 6H, $AlCH_3$), 2.41 (s, 6H, NCH_3), 0.13 (s, 18H, $SiCH_3$). ^{13}C-NMR (**1a**): δ −6.0 ($AlCH_3$), 33.68 (NCH_3), 0.53 ($SiCH_3$); ^{13}C-NMR (**1b**): δ −9.1 ($AlCH_3$), −3.2 ($AlCH_3$), 35.46 (NCH_3), 0.53 ($SiCH_3$).

2.5.2. $[Me_2GaN(Me)SiMe_3]_2$ (**2**)

M.p. 69–73°C, 90% yield. ^{1}H-NMR (**2a**): δ −0.11 (s, 12H, $GaCH_3$), 2.38 (s, 6H, NCH_3), 0.11 (s, 18H, $SiCH_3$); ^{1}H-NMR (**2b**): δ −0.17 (s, 6H, $GaCH_3$), 0.00 (s, 6H, $GaCH_3$), 2.47 (s, 6H, NCH_3), 0.094 (s, 18H, $SiCH_3$). ^{13}C-NMR (**2a**): δ −3.93 ($GaCH_3$), 35.56 (NCH_3), 0.39 ($SiCH_3$); ^{13}C-NMR (**2b**): δ −7.34 ($GaCH_3$), −0.65 ($GaCH_3$), 37.47 (NCH_3), 0.39 ($SiCH_3$). IR (cm^{-1}): 2979 (m), 2951 (m), 2896 (w), 1264 (s), 1252 (vs), 1202 (m), 987 (s), 843 (vs), 761 (vs), 725 (vs), 559 (m), 504 (s). Calc. MW: 404.04 g mol^{-1}, Cryoscopic MW: 415 g mol^{-1} (average of three determinations, $m = 0.0495$). Anal. Calc. for $C_{12}H_{36}Ga_2N_2Si_2$: C, 35.67; H, 8.98; N, 6.93. Found: C, 35.81; H, 8.60; N, 6.96%.

2.5.3. $[Me_2InN(Me)SiMe_3]_2$ (**3**)

M.p. 76–78°C, 92% yield. ^{1}H-NMR (**3a**): δ −0.022 (s, 12H, $InCH_3$), 2.58 (s, 6H, NCH_3), 0.083 (s, 18H, $SiCH_3$). ^{1}H-NMR (**3b**): δ −0.072 (s, 6H, $InCH_3$), 0.077 (s, 6H, $InCH_3$), 2.66 (s, 6H, NCH_3), 0.083 (s, 18H, $SiCH_3$). ^{13}C-NMR (**3a**): δ −5.60 ($InCH_3$), 36.65 (NCH_3), 0.28 ($SiCH_3$). ^{13}C-NMR (**3b**): δ −8.71 ($InCH_3$), −2.32 ($InCH_3$), 38.18 (NCH_3), 0.28 ($SiCH_3$). IR (cm^{-1}): 2946 (m), 2919 (m), 2886 (m), 1251 (s), 1161 (m), 1143 (m), 984 (s), 818 (vs), 750 (m), 710 (s), 490 (w), 456 (s). Anal. Calc. for $C_{12}H_{36}In_2N_2Si_2$: C, 29.16; H, 7.34; N, 5.67. Found: C, 29.21; H, 7.13; N, 5.53%.

2.6. Crystallographic data for **3a**

X-ray quality crystals of **3a** were obtained by recrystallization of the compound from toluene at −15°C. A single crystal was sealed in a thin-walled capillary under nitrogen. Molecular structure data were acquired using an Enraf–Nonius CAD4 diffractometer with κ-geometry using Mo–K_α radiation ($\lambda = 0.71073$ Å). Data were collected by a coupled ω–2θ scan method. Refinement procedures were carried out using the SHELXTL-PC program package [23]. The structure was solved using Patterson synthesis. Positional and anisotropic thermal parameters were refined for all non-hydrogen atoms. Hydrogen atoms were placed in calculated positions with the appropriate staggered geometry. The U_{eq} of each hydrogen atom was set equal to that of the carbon atom to which it was bound. Refinement continued until convergence was reached with the mean $\Delta/\sigma < 0.01$. Upon convergence, no chemically significant residuals were observed in the final difference-Fourier synthesis. Further details of the data collection and refinement processes are provided in Table 1. Selected bond lengths (Å) and angles (°) are given in Table 2.

3. Results and discussion

3.1. Study of the donor capacity of silylamines

A compilation of the differences in the ^{1}H- and ^{13}C-NMR chemical shifts (ppm) between each 1:1 mole

Table 1
Crystal data for *trans*-$[Me_2InN(Me)SiMe_3]_2$

Formula	$C_{12}H_{36}In_2N_2Si_2$
Space group	$P2_1/n$
Crystal system	Monoclinic
Temperature (K)	294
a (Å)	8.7735(22)
b (Å)	11.2984(20)
c (Å)	11.2006(17)
β (°)	90.635(17)
V (A^3)	1110.2(6)
Z	4
Crystal size (mm)	$0.30 \times 0.20 \times 0.20$
Absorption coefficient (mm^{-1})	2.176
Radiation, λ (Å)	Mo–K_α, 0.71073
2θ range (°)	2.0–45.0
Scan type	$\omega-2\theta$
Index ranges	$0 \le h \le 9$, $-12 \le k \le 12$, $-12 \le l \le 12$
Reflections collected	3022
Independent reflections	1451 [$R_{int} = 2.73$]
Observed reflections	974 [$F > 6.0\sigma(F)$]
R indices (all data)	$R = 4.34$, $Rw = 3.96$
R indices (6σ data)	$R = 2.40$, $Rw = 3.42$
Largest difference peak and hole (e A^{-3})	0.50 and −0.31

Table 2
Selected bond lengths (Å) and angles (°) for *trans*-[$Me_2InN(Me)SiMe_3]_2$

In(1)–N(1)	2.251(3)	In(1)–C(1)	2.144(5)
In(1)–C(2)	2.142(5)	In(1)···In(1A)	3.283(1)
In(1)–N(1A)	2.247(3)	N(1)–C(3)	1.508(6)
N(1)–Si(1)	1.742(4)	N(1)–In(1A)	2.247(3)
N(1)–In(1)–N(1A)	86.2(1)	C(1)–In(1)–C(2)	118.7(2)
In(1)–N(1)–In(1A)	93.8(1)	C(3)–N(1)–Si(1)	110.7(3)

ratio mixture and the respective reactants in terms of the Me–M, the Si–Me, and the N–Me methyl group resonances is given in Table 3. For the Ga and In adducts, the ^{13}C-NMR chemical shifts of the Me–M groups move upfield significantly for the two monosilylated amines, comparable to those for the Me_3Ga and Me_3In adducts with Me_2NH [15] and other secondary alkyl amines (No comparison can be made with trimethylaluminum as it exists as a dimer in benzene solution). No significant changes are noted in the Me–M ^{13}C-NMR chemical shifts for mixtures involving $N(SiMe_3)_3$, $HN(SiMe_3)_2$, and $NMe(SiMe_3)_2$. Similarly, there are only meaningful ^{1}H- and ^{13}C-NMR chemical shift changes for the methyl resonances in the trimethylsilyl group for mixtures of Me_3Al, Me_3Ga, and Me_3In with the two monosilylated amines. Finally, the ^{1}H- and ^{13}C-NMR chemical shift differences for the methyl resonances in the N–Me group upon adduct formation for the monosilylated amines $HN(Me)SiMe_3$ and $N(Me)_2SiMe_3$ are comparable to those for $HNMe_2$. These NMR data clearly show that there are significant changes in the ^{13}C- and ^{1}H-NMR chemical shifts between the mixtures and the starting reagents, indicative of strong adduct formation, only when the amine contains one trimethylsilyl group. These results are consistent with studies on the relative electron donor ability and basicity of monosilylated alkylamines versus alkylamines toward Lewis acids from classical [24–26] as well as IR and electronic spectroscopic [27] and ^{1}H-NMR chemical shift [28] studies.

Because the changes in the ^{1}H- and ^{13}C-NMR chemical shifts for the secondary amine, $HN(Me)SiMe_3$, upon adduct formation with Me_3Al, Me_3Ga, and Me_3In are comparable with those for the previously reported series of secondary alkylamines [9,15], we used the previously reported correlations between ^{13}C-NMR Me–M chemical shifts and amine cone angle to estimate the cone angle for this amine. The average calculated value from the three data is $129.8 \pm 1.2°$. This estimated value seems reasonable because the literature value of the cone angle for $HNMe_2$ is 119°. Furthermore, because the cone angles of H_3N, H_2NMe, $HNMe_2$, and NMe_3 are 94, 106, 119, and 132° [29], respectively, a simple calculation suggests that replacement of a hydrogen by a methyl group on a given amine increases the cone angle by ca. 12°. From these

Table 3
Changes in chemical shifts upon mixing ($\Delta\delta = \delta(\text{mixture}) - \delta(\text{free})$)

	^{1}H			^{13}C		
Bound amine	Al	Ga	In	Al	Ga	In
M–Me shift differences (ppm)						
$N(SiMe_3)_3$	[0.00] [a]	0.00	−0.02	[0.04] [a]	0.03	−0.05
$HN(SiMe_3)_2$	– [b]	0.00	−0.02	– [b]	0.02	−0.09
$NMe(SiMe_3)_2$	[−0.01] [a]	0.00	−0.07	[0.50] [a]	0.02	−0.10
$HN(Me)SiMe_3$	[−0.20] [a]	−0.06	0.09	[0.13] [a]	−5.49	−6.11
$N(Me)_2SiMe_3$	[−0.21] [a]	−0.06	0.08	[−0.48] [a]	−5.40	−5.15
$HNMe_2$	[−0.23] [a]	−0.14	0.05	[−2.51] [a]	−5.85	−8.54
Si–Me shift differences (ppm)						
$N(SiMe_3)_3$	0.00	0.00	0.00	0.00	−0.01	−0.01
$HN(SiMe_3)_2$	– [b]	0.00	0.01	– [b]	0.01	−0.03
$NMe(SiMe_3)_2$	0.00	0.00	0.01	0.02	0.00	−0.03
$HN(Me)SiMe_3$	−0.14	−0.10	−0.11	−1.11	−0.82	−0.91
$N(Me)_2SiMe_3$	−0.11	−0.10	−0.11	−1.39	−1.08	−1.67
N–Me shift differences (ppm)						
$NMe(SiMe_3)_2$	−0.04	0.00	−0.01	0.34	0.01	0.01
$HN(Me)SiMe_3$	−0.55	−0.55	−0.32	1.35	1.64	0.97
$N(Me)_2SiMe_3$	−0.51	−0.46	−0.38	1.79	1.95	1.75
$HNMe_2$	−0.69	−0.64	−0.62	−2.37	−1.91	−1.24

[a] Derived using $(Me_3Al)_2$ data.
[b] 1,2-elimination occurs above 0°C.

data, the cone angle of the bound $N(Me)_2SiMe_3$ is estimated to be 142°. Due to the absence of any internal degrees of freedom to reduce the cone angle of the bound silylamines, these values should be representative of those of the free silylamines.

Low-temperature data at −33°C gave no indication of complexation in the Me_3M-polysilylated amine mixtures. NMR chemical shift studies showed no evidence of dissociation of the Me_3M-monosilylated amine adducts up to 63°C.

3.2. Thermodynamic and kinetics studies of the equilibration of trans to cis forms of $[Me_2MN(Me)SiMe_3]_2$ where M = Al, Ga, In

Thermolysis of the adducts, $Me_3M{\cdot}HN(Me)SiMe_3$, where M = Al, Ga, and In, leads in each case to the respective dimer, $[Me_2MN(Me)SiMe_3]_2$. The synthesis of $[Me_2AlN(Me)SiMe_3]_2$ (**1**) has been reported and **1** was found to be dimeric in benzene solution by cryoscopic molecular weight determinations [21,22]. From cryoscopy studies in benzene solution $[Me_2GaN(Me)SiMe_3]_2$ (**2**) was found to be dimeric in this study. $[Me_2InN(Me)SiMe_3]_2$ (**3**) is dimeric in the solid state and exists in a *trans* configuration as evidenced by the molecular structure determined from X-ray single crystal studies, discussed below.

Due to the unsymmetric nature of the amine, the three dimers could exist in solution in either the *cis* or the *trans* conformation with respect to the four-membered ring, or as a mixture of the two. In the *trans* conformation, the Me–M, the N–Me, and the $SiMe_3$ resonances should exhibit only one resonance each in the ^{1}H- and ^{13}C-NMR spectra, due to the symmetry present, while for the *cis* conformation, there should be two resonances present for the Me–M group. The results of previous 60 MHz ^{1}H-NMR studies reported that $[Me_2AlN(Me)SiMe_3]_2$ exists exclusively in the *trans* conformation in benzene-d_6 solution [30]. Recrystallization of **1**, **2**, and **3** from toluene yields only the *trans* form of each dimer as evidenced by ^{1}H-NMR data. ^{1}H-NMR data obtained as rapidly as possible after preparation of the sample in benzene-d_6 solution show one dominant set of resonances assignable to the *trans* isomer, and a trace of resonances attributable to the *cis* isomer, which grow at the expense of the *trans* resonances with time. The ^{1}H- and ^{13}C-NMR chemical shift assignments are trivial for the *trans* and *cis* isomers of **1**, **2**, and **3**, except for the assignment of the two Me–M resonances in the *cis* isomer. The ^{1}H-NMR chemical shift assignments were made from ^{1}H 2-D Noesy experiments. The upfield Me–M resonance in each of the three *cis* dimers showed a correlation with the ^{1}H-NMR resonance of the N–Me group, suggesting that the upfield resonance belongs to the methyl group on the same side of the $[MN]_2$ ring as the N–Me group.

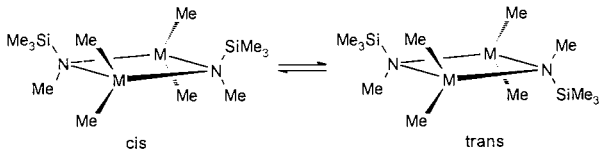

Scheme 1. *Cis–trans* isomerization for $[Me_2MN(Me)SiMe_3]_2$ where M = Al, Ga, and In.

Assignments of the Me–M ^{13}C-NMR resonances were then determined from $^{13}C\{^1H\}$ 2-D heteronuclear correlated spectroscopy (Scheme 1).

The kinetics of interconversion of $[Me_2MN(Me)SiMe_3]_2$ from a *trans* conformation to a *trans*/*cis* equilibrium mixture at r.t. depends on the metal, with the rates being in the order **3** > **2** ≫ **1** or In > Ga ≫ Al. Other equilibria, which could give multiple resonances in the NMR spectrum such as dimer–trimer equilibrium, were ruled out due to the concentration independence of the ^{1}H- and ^{13}C-NMR spectra of the compounds. Similar equilibrium mixtures of *cis* and *trans* dimers in solution have been reported for aminoalanes, aminogallanes, and aminoindanes by ^{1}H-NMR spectroscopy, including $[Me_2MN(Me)Ph]_2$, where M = Al, Ga, and In [18]; $[Me_2MN(H)Bu^t]_2$, where M = Al and Ga [19,20]; $[Et_2AlN(R)SiMe_3]_2$, where R = Me, Ph, and Pr^i [30]; $[Me_2AlN(H)SiR_3]_2$, where R = Me, Et, and Ph [31]; $[Me_2AlN(H)Pr^i]_2$ [32]; and $[Et_2AlN(H)Bu^t]_2$ [33].

The *trans* to *cis* isomerization process for each dimer was studied as a function of temperature and time by ^{1}H-NMR spectroscopy. Relative concentrations of the two isomers were determined at a given temperature and time by monitoring the integral ratios of the peaks due to the $N–CH_3$ group. The $N–CH_3$ group gives a single resonance for each isomer in each system, where the resonances are well separated from each other and from other resonances in the respective dimer. Due to the different isomerization rates at a given temperature for the three systems, the data were taken over different temperature ranges for each system as noted in Table 4. Analysis of the kinetic data showed a reversible first-order process for the isomerization and approach to equilibrium for all three systems. The kinetic data for **2** are plotted at several temperatures in Fig. 1. Because the data fit a reversible first-order kinetic model, the individual rate constants for the forward (k_1) and reverse (k_{-1}) processes can be obtained from the equilibrium constant [$K_{eq} = k_1/k_{-1}$] and the slope of the reversible first-order plot (where the slope is the sum of k_1 and k_{-1}). The model was tested further by performing *trans* to *cis* isomerization studies for 0.050 M solutions of **2** and **3** at 305.8 K. The kinetic and thermodynamic data were consistent with the previous 0.10 M data, suggesting an intramolecular process. Additionally, 'crossover' experiments were performed

Table 4
Kinetic data (min^{-1}) in toluene-d_8 solution

	Ga (**2**)			In (**3**)		
T (K)	$k_{obs} \times 10^3$	$k_1 \times 10^3$	$k_{-1} \times 10^3$	$k_{obs} \times 10^3$	$k_1 \times 10^3$	$k_{-1} \times 10^3$
305.8	0.93(3)	0.24(2)	0.69(2)	5.79(6)	1.75(2)	3.95(4)
311.3	2.27(4)	0.61(1)	1.66(3)	10.5(1)	3.20(3)	7.30(7)
316.8	5.01(4)	1.38(1)	3.62(3)	26.9(3)	8.44(9)	18.5(2)
322.5	9.33(8)	2.53(2)	6.48(6)	42.4(13)	13.5(4)	28.9(9)
327.5	19.5(3)	5.43(9)	13.6(2)	78.0(23)	24.8(7)	53.2(16)
332.5	52.2(13)	15.1(4)	36.9(9)			
338.2	98.9(33)	29.3(10)	69.7(23)			
	Al (**1**)					
	$k_{obs} \times 10^3$	$k_1 \times 10^3$	$k_{-1} \times 10^3$			
343.0	0.143(4)	0.041(1)	0.100(3)			
348.9	0.243(4)	0.072(1)	0.171(3)			
353.8	0.516(6)	0.152(2)	0.358(4)			
359.5	1.07(1)	0.322(3)	0.750(7)			
364.0	2.01(2)	0.607(6)	1.40(1)			

by mixing 0.20 M solutions of **2** and **3** and collecting ^{1}H-NMR spectra as a function of time at 305.8 K. No new resonances were observed in the spectra.

The kinetic rate constants for the three systems are given at several temperatures in Table 4 and the corresponding equilibrium constants in Table 5. The magnitude of K_{eq} indicates that the *trans* isomer is favored at all the investigated temperatures, but that the relative amount of *cis* isomer increases with increasing temperature. Due to the very slow rate of isomerization of **1**, K_{eq} values could only be obtained at high temperatures. The calculated thermodynamic data for the isomerization processes in **1**, **2**, and **3** are given in Table 6. The *trans* isomer is thermodynamically more stable, but the positive entropy term favors the *cis* isomer, as expected due to lower symmetry, similar to that in the isomerization studies of *trans* to *cis* $[Me_2GaN(H)Bu^t]_2$ ($\Delta H° = 3.12$ kJ mol^{-1}; $\Delta S° = 4.56$ J mol^{-1} K) [19], and $[Me_2AlN(H)Bu^t]_2$ ($\Delta H° = 2.22$ kJ mol^{-1}; $\Delta S° = 2.85$ J mol^{-1} K) [20]. The *cis*/*trans* ratio of about 0.40 for **1** is consistent with the 30–35% *cis* reported for $[Et_2AlN(Me)SiMe_3]_2$ in benzene-d_6 solution at r.t. [30].

The similarity of the thermodynamic data for the three systems as well as similar *cis*/*trans* ratios at a given temperature in benzene-d_6 or toluene-d_8 solutions suggest that *cis*–*trans* interconversion may occur by the same mechanistic processes for **1**, **2**, and **3**. This is in contrast to the results published for the solution properties of $[Me_2MN(Me)Ph]_2$, where M = Al, Ga, and In [18]. Here, the observed *cis*/*trans* ratio decreases in the order Al > Ga > In. For the aluminum and gallium compounds, the *cis* isomer predominates whereas the *trans* isomer is more abundant for the indium derivative. In the solid state $[Me_2InN(Me)Ph]_2$ was found to exist in a *trans* conformation from single crystal X-ray data. The *cis*/*trans* isomer ratio decreases with increasing temperature for the aluminum and indium dimers, but increases with temperature for the gallium dimer.

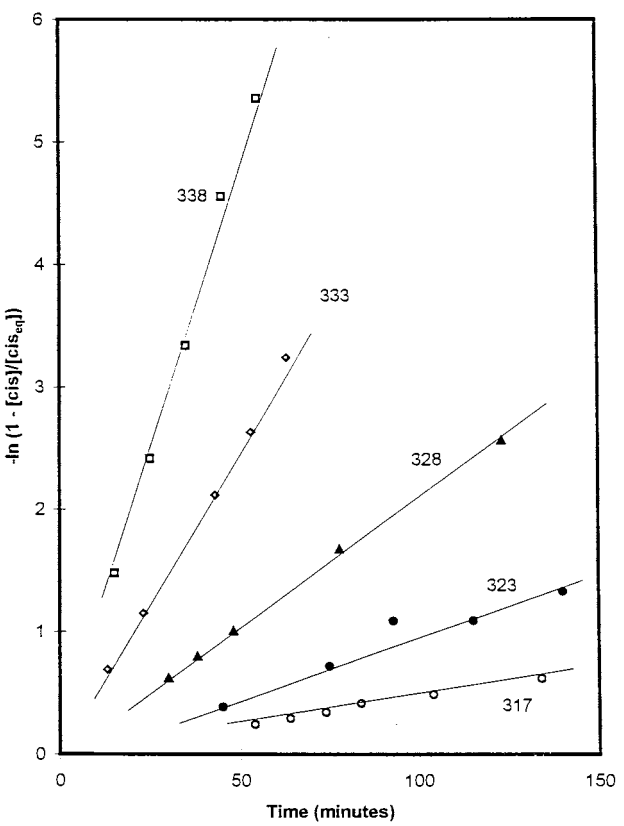

Fig. 1. Reversible first-order kinetics plots of the isomerization of **2** in toluene-d_8 solution at several temperatures (K).

Table 5
Equilibrium constants as a function of temperature in toluene-d_8 solution

T (K)	Al (**1**)	Ga (**2**)	In (**3**)
305.8		0.360(1)	0.444(7)
316.8		0.381(5)	0.457(2)
322.5		0.391(5)	0.465(7)
327.5		0.398(7)	0.467(2)
332.5		0.406(5)	0.479(3)
338.2		0.417(3)	0.485(3)
348.9			0.489(4)
359.5	0.428(10)		
364.0	0.434(5)		
368.9	0.441(4)		

Activation parameters for the *trans* to *cis* interconversion process were calculated from an Eyring analysis of the rate constant versus temperature data. The enthalpies and entropies of activation for the forward and reverse processes were obtained from plots of $\ln(k_1/T)$ versus $1/T$ and of $\ln(k_{-1}/T)$ versus $1/T$ and are given in Table 6 for **1**, **2**, and **3**. The difference, $\Delta H_1 - \Delta H_{-1} = \Delta H°$, is in good agreement with $\Delta H°$ determined from the thermodynamic studies. The mechanism [17,19,20,31,34] that has been proposed for related systems, in which the interconversion has been shown to be concentration independent and intramolecular, involves an initial breaking of an M–N bond, followed by rotation about the nonbridged M–N bond and rebridging. This is reasonable in terms of the reported enthalpies of adduct formation of Me_3N to Me_3M of -125, -88, and -83 kJ mol^{-1} for M = Al, Ga, and In, respectively [35]. Such a mechanism would imply that the enthalpies of activation would decrease in the order Al > Ga > In, or the inverse of the observed magnitudes of the rate constants. While such an ordering is present, the ΔH_1 and ΔH_{-1} values for **1** and **2** are too close in magnitude for the energetics of M–N bond breaking to explain the large differences in forward and reverse rate constants for the aluminum and gallium systems. The difference in the kinetic parameters for isomerization of **1** and **2** must arise from the entropy of activation term where the larger positive entropy of activation term for the $[Me_2GaN(Me)SiMe_3]_2$ is responsible for the faster isomerization process as compared to $[Me_2AlN(Me)SiMe_3]_2$. Two possible explanations are suggested by these data. The first is the existence of a sterically congested transition state for **1**, which is not as probable in **2**, due to the longer Ga–N versus Al–N bond lengths in aminogallanes compared to aminoalanes [36–39]. Secondly, trialkylaluminum species and aminoalane dimers can interact strongly with aromatic solvents, forming solvent-collision complexes, which can lower the rates of the kinetic processes by decreasing the magnitude of the entropy of activation term for *trans–cis* isomerization in **1** [18,20,39–41].

Table 6
Thermodynamic data and kinetic activation parameters in toluene-d_8 solution

	Al (**1**)	Ga (**2**)	In (**3**)
$\Delta H°$	3.31(0.14) kJ mol^{-1}	4.22(0.06) kJ mol^{-1}	2.08(0.15) kJ mol^{-1}
$\Delta S°$	2.17(0.39) J mol^{-1}	5.26(0.20) J mol^{-1}	0.783(0.11) J mol^{-1}
ΔH_1	132.9(5.2) kJ mol^{-1}	130.2(8.9) kJ mol^{-1}	100.2(5.8) kJ mol^{-1}
ΔS_1	56.80(1.76) J mol^{-1}	109.6(3.3) J mol^{-1}	29.60(2.20) J mol^{-1}
ΔH_{-1}	130.6(5.2) kJ mol^{-1}	125.9(8.8) kJ mol^{-1}	97.70(5.44) kJ mol^{-1}
ΔS_{-1}	57.27(1.76) J mol^{-1}	104.3(3.2) J mol^{-1}	28.43(2.07) J mol^{-1}

Kinetic parameters for the *trans* to *cis* interconversion have also been obtained for $[Me_2GaN(H)Bu^t]_2$ [19] and $[Me_2AlN(H)Bu^t]_2$ [20]. The enthalpies of activation for the aminogallane are $\Delta H_1 = 120.8$ and $\Delta H_{-1} = 117.8$ kJ mol^{-1}, in excellent agreement with the data for **2**. The entropies of activation, $\Delta S_1 = 41.4$ and $\Delta S_{-1} = 37.3$ J mol^{-1} K^{-1}, are lower than the value for **2**. However, this aminogallane contains a primary amine fragment as opposed to a secondary amine fragment in **2**. The enthalpies and negative entropies of activation reported for $[Me_2AlN(H)Bu^t]_2$ are inconsistent with our results for **1** and also with data on $[Me_2GaN(H)Bu^t]_2$. Lower than expected enthalpies and negative entropies of activation have been published for intramolecular *cis–trans* isomerization processes in organometallic complexes in benzene solution where these effects have been attributed to aromatic solvent-collision complexes [42,43].

3.3. Crystal structure of trans-$[Me_2InN(Me)SiMe_3]_2$

The ORTEP drawing of the molecular structure and the atom labeling scheme of **3a** are shown in Fig. 2. The X-ray crystal structures of related aminoindane dimers, $[Me_2InR]_2$, where R = NMe_2 [44] and NEt_2, NPr^i_2, and $N(SiMe_3)_2$ [45] have been reported. The molecular structures for these compounds possess a central planar In_2N_2 ring with dimensions similar to that for **3a**. The molecular parameters for this series of compounds were analyzed in terms of the change in molecular geometry with respect to the increase in steric bulk of the ligand attached to the nitrogen atom [45]. There were several trends in the change in molecular geometry of the In_2N_2 ring with substituent, including the lengthening of the In–N bond with increasing steric bulk. The In–N bond lengths for $[Me_2InNMe_2]_2$ are 2.22(2) Å, while those for $[Me_2InN(SiMe_3)_2]_2$ are 2.304(5) and 2.305(5) Å. Also, with increasing steric bulk, there is an increase in the

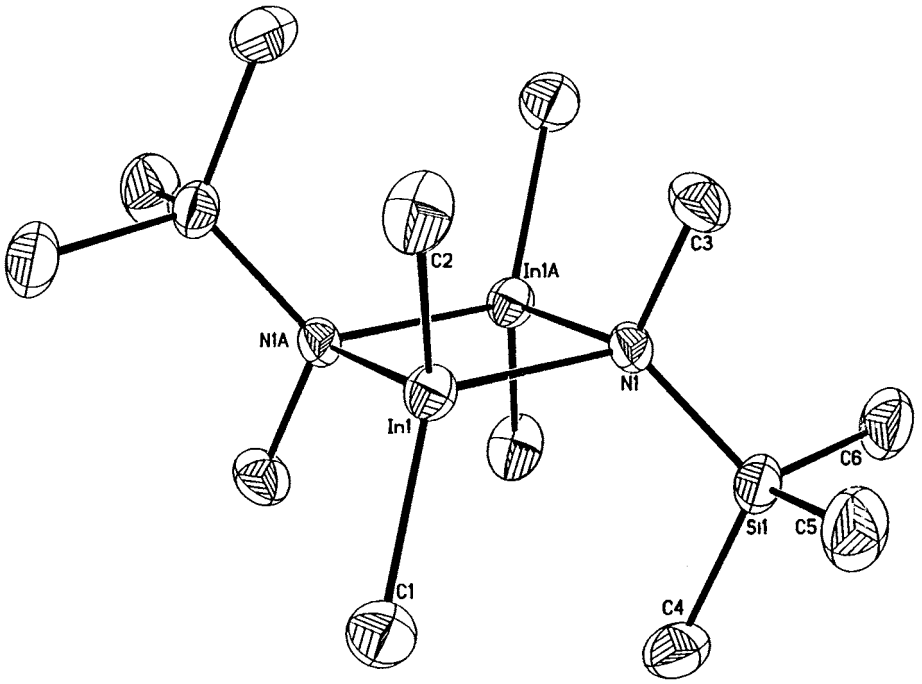

Fig. 2. Molecular structure and atom numbering scheme for *trans*-$[Me_2InN(Me)SiMe_3]_2$.

N–In–N angle ($R = NMe_2$, 85.7(4); $R = N(SiMe_3)_2$, 89.7(1)°) with a corresponding decrease in the In–N–In angle ($R = NMe_2$, 94.3(3); $R = N(SiMe_3)_2$, 90.3(1)°). The external C–In–C angle decreases considerably in the series from 131.3(4) for $R = NMe_2$ to 109.1(1)° for $R = N(SiMe_3)_2$. In this series increasing steric bulk in the amido group is accommodated by small increases in the In–N distances as well as small changes in the internal ring angles and significant decreases in the C–In–C bond angles.

Comparison of the molecular parameters for **3a** listed in Table 2 with those of $[Me_2InNMe_2]_2$ and $[Me_2InN(SiMe_3)_2]_2$ suggest that substitution of one trimethylsilyl group for a methyl group causes only small changes in the In_2N_2 central ring bond angles and distances. The steric strain caused by the introduction of the more bulky substituent is relieved by a significant decrease in the C–In–C bond angle. However, substitution of a second trimethylsilyl moiety causes larger changes in ring geometry, as well as a continued decrease in the C–In–C bond angle.

4. Supplementary material

Tables of crystallographic data, data collection and structure refinement details have been deposited with the Cambridge Crystallographic Data Centre, CCDC-113673 for the compound *trans*-$[Me_2InN(Me)SiMe_3]_2$.

Acknowledgements

This work was supported in part by a US Department of Education GAANN Fellowship to E.K.S.

References

[1] J.J. Eisch, in: G. Wilkinson, F.G.A. Stone, E.W. Abel (Eds.), Comprehensive Organometallic Chemistry, vol. 2, Pergamon Press, Oxford, 1982.
[2] T. Mole, E. Jeffery, Organoaluminium Compounds, Elsevier, Amsterdam, 1972, Ch. 4.
[3] G.E. Coates, M.L.H. Green, K. Wade, Organometallic Compounds, 3rd ed., vol. 1, Methuen, London, 1967, Ch. 3.
[4] A. McKillop, J.D. Smith, I.J. Worrall, Organometallic Compounds of Aluminum, Gallium, and Indium, Chapman and Hall, London, 1985.
[5] A. Haaland, in: G.H. Robinson (Ed.), Coordination Chemistry of Aluminum, VCH, New York, 1993, Ch. 1.
[6] N. Davidson, H.C. Brown, J. Am. Chem. Soc. 64 (1942) 316.
[7] G.E. Coates, J. Chem. Soc. (1951) 2003.
[8] G.E. Coates, R.A. Whitcombe, J. Chem. Soc. (1956) 3351.
[9] C.J Thomas, L.K. Krannich, C.L. Watkins, Polyhedron 12 (1993) 389.
[10] B. Sen, G.L. White, J. Inorg. Nucl. Chem. 35 (1973) 2207.
[11] C.H. Hendrickson, D. Duffy, D.P. Eyman, Inorg. Chem. 7 (1968) 1047.
[12] M. Taghiof, D.G. Hendershot, M. Barber, J.P. Oliver, J. Organomet. Chem. 431 (1992) 271.
[13] D.C. Bradley, H.M. Dawes, M.B. Hursthouse, L.M. Smith, M. Thornton-Pett, Polyhedron 9 (1990) 343.
[14] D.C. Bradley, H. Dawes, D.M. Frigo, M.B. Hursthouse, B.J. Hussain, J. Organomet. Chem. 325 (1987) 55.
[15] S.J. Schauer, C.L. Watkins, L.K. Krannich, R.B. Gala, E.M. Gundy, C.B. Lagrone, Polyhedron 14 (1995) 3505.

[16] A.R. Barron, J. Chem. Soc. Dalton Trans. (1988) 3047.
[17] K. Wakatsuki, T. Tanaka, Bull. Chem. Soc. Jpn. 48 (1975) 1475.
[18] O.T. Beachley Jr., C. Bueno, M.R. Churchill, R.B. Hallock, R.G. Simmons, Inorg. Chem. 20 (1981) 2423.
[19] J.T. Park, Y. Kim, J. Kim, K. Kim, Y. Kim, Organometallics 11 (1992) 3320.
[20] J.T. Park, W.T. Oh, Y. Kim, Bull. Korean Chem. Soc. 17 (1996) 1147.
[21] T. Sakakibara, T. Hirabayashi, Y.J. Ishii, J. Organomet. Chem. 46 (1972) 231.
[22] G. Sonnek, M. Päch, H. Bredereck, L. Oswald, J. Organomet. Chem. 329 (1987) 31.
[23] Siemens SHELXTL-PC Manual, Release 4.1, Siemens Analytical Instruments, Madison, WI, 1990.
[24] A.W. Jarvie, D. Lewis, J. Chem. Soc. (1963) 1073.
[25] E.A.V. Ebsworth, H.J. Emeleus, J. Chem. Soc. (1958) 2150.
[26] S.W. Jarvie, D. Lewis, J. Chem. Soc. (1963) 4758.
[27] K.J. Fisher, C.E. Ezeani, Polyhedron 2 (1983) 393.
[28] G. Sonnek, M. Päch, Z. Chem. 26 (1986) 259.
[29] A.L. Seligson, W.C. Trogler, J. Am. Chem. Soc. 113 (1991) 2520.
[30] G. Sonnek, M. Päch, J. Prakt. Chem. 329 (1987) 907.
[31] D.M. Choquette, M.J. Timm, J.L. Hobbs, M.M. Rahim, K.J. Ahmed, R.P. Planalp, Organometallics 11 (1992) 529.
[32] S. Amirkhalili, P.B. Hitchcock, A.D. Jenkins, J.Z. Nyathi, J.D. Smith, J. Chem. Soc. Dalton Trans. (1981) 377.
[33] K. Gosling, J.D. Smith, D.H.W. Wharmby, J. Chem. Soc. A (1969) 1738.
[34] A.M. Arif, D.C. Bradley, H. Dawes, D.M. Frigo, M.B. Hursthouse, B. Hussain, J. Chem. Soc. Dalton Trans. (1987) 2159.
[35] K.B. Starowieyski, in: A.J. Downs (Ed.), Chemistry of Aluminium, Gallium, Indium, and Thallium, Chapman and Hall, London, 1993, Ch. 6.
[36] S.J. Schauer, C.H. Lake, C.L. Watkins, L.K. Krannich, D.H. Powell, J. Organomet. Chem. 549 (1997) 31.
[37] W.R. Nutt, K.J. Murry, J.M. Gulick, J.D. Odom, Y. Ding, L. Lebioda, Organometallics 15 (1996) 1728.
[38] S.J. Schauer, G.H. Robinson, J. Coord. Chem. 30 (1993) 197.
[39] D.C. Bradley, I.S. Harding, I.A. Maia, M. Motevalli, J. Chem. Soc. Dalton Trans. (1997) 2969.
[40] O.T. Beachley Jr., C. Tessier-Youngs, Inorg. Chem. 11 (1979) 3188.
[41] T.L. Brown, Acc. Chem. Res. 1 (1968) 23.
[42] Y. Kawano, H. Tobita, H. Ogino, Organometallics 11 (1992) 499.
[43] M.I. Altbach, C.A. Muedas, R.P. Korswagen, M.L. Ziegler, J. Organomet. Chem. 306 (1986) 375.
[44] K. Mertz, W. Schwarz, B. Eberwein, J. Weidlein, H. Hess, H.D. Hausen, Z. Anorg. Allg. Chem. 429 (1977) 99.
[45] K.A. Aitchison, J.D. Backer-Dirks, D.C. Bradley, M.M. Faktor, D.M. Frigo, M.B. Hursthouse, B. Hussain, R.L. Short, J. Organomet. Chem. 366 (1989) 11.